# Correlation of Vortex Motion in High-$T_c$ Superconductors

Thomas S. Lee,[1] N. Missert,[1,*] Lise T. Sagdahl,[1,†] John Clarke,[1] John R. Clem,[2] K. Char, [3] J. N. Eckstein,[4] D. K. Fork,[5] L. Lombardo,[6] A. Kapitulnik,[6] L. F. Schneemeyer,[7] J. V. Waszczak,[7] and R. B. van Dover[7]

[1]*Department of Physics, University of California, Berkeley, California 94720 and Materials Science Division, Lawrence Berkeley Laboratory, Berkeley, California 94720*

[2]*Ames Laboratory and Department of Physics and Astronomy, Iowa State University, Ames, Iowa 50011*

[3]*Conductus Incorporated, Sunnyvale, California 94086*

[4]*Varian Research Center, Palo Alto, California 94304*

[5]*Xerox Palo Alto Research Center, Palo Alto, California 94304*

[6]*Department of Applied Physics, Stanford University, Stanford, California 94305*

[7]*AT&T Bell Laboratories, Murray Hill, New Jersey 07974*

(Received 12 September 1994)

The magnetic flux noise generated by films and crystals of $Bi_2Sr_2CaCu_2O_{8+y}$ and $YBa_2Cu_3O_{7-x}$, up to 30 $\mu$m thick and cooled in nominally zero magnetic field, has been measured at opposing surfaces by two dc superconducting quantum interference devices. For both materials, the noise sources at the two surfaces were highly correlated at specific temperatures in a given cooldown. This result suggests that the observed vortices moved as rigid rods. At other temperatures, the noise was mostly uncorrelated, suggesting that the relevant vortices were pinned at more than one point along their length.

PACS numbers: 74.60.Ge, 74.40.+k, 74.72.Bk, 74.72.Hs

Understanding the internal structure of magnetic flux vortices in superconductors is of great scientific and technological importance. For example, the intrinsic rigidity of a flux vortex greatly determines how effectively it can be immobilized by a pinning site. A flux vortex in isotropic, conventional low transition temperature ($T_c$) superconductors is typically modeled as a continuous rigid rod. In contrast, the internal structure of flux vortices in the high-$T_c$ superconductors (HTSC) is strongly influenced by the anisotropy of these layered materials. In particular, each vortex along the $c$ axis may be considered as a stack of two-dimensional pancake vortices which are confined to the $CuO_2$ planes [1–4]. This implies that vortices in the HTSC may be significantly less rigid than their low-$T_c$ counterparts and, therefore, more susceptible to thermally driven motion.

In the absence of flux pinning and thermal fluctuations, the coupling between each pair of pancake vortices in the HTSC is determined by magnetic and Josephson coupling [1–7]. This net interlayer coupling has been investigated in the HTSC by experiments in the mixed state [8–10] in which a magnetic field (~1 T) was applied along the $c$ axis of a crystal and a current injected along one surface in the $ab$ direction. In the case of $Bi_2Sr_2CaCu_2O_{8+y}$ (BSCCO) [8,9], it was found that the voltage drop across the surface with the current contacts greatly exceeded that across the opposing surface, implying that the vortices were sheared by the strong Lorentz force exerted by the current. In contrast, in $YBa_2Cu_3O_{7-x}$ (YBCO) the voltages on the two sides of a YBCO crystal [10] were identical below a characteristic temperature, implying that the vortices moved as rigid rods. These findings are consistent with the theoretical prediction that the total coupling energy between pancakes in adjacent layers in YBCO is at least 50 times greater than that in BSCCO [1–7]

In this Letter we examine the rigidity of individual thermally generated vortices in the previously unexplored limits of the nominally zero applied magnetic field ($<10^{-7}$ T) and zero driving current. In contrast to the above transport current studies, these experimental conditions allow us to investigate the dynamics of isolated vortices moving only under thermal activation and without the shearing forces exerted by a driving current. We use two dc superconducting quantum interference devices (SQUIDs), one above and one below a film or crystal of YBCO and BSCCO, to measure the temporal correlation of the magnetic flux noise generated at the two surfaces. From the degree of correlation we infer the extent to which the motion of the ends of a given vortex is coherent, thereby providing a measure of its apparent rigidity.

In our experiment, two thin film, Nb-PbIn dc SQUIDs, $A$ and $B$ [11] were mounted about 100 $\mu$m away from the two opposing sides of the sample [inset, Fig. 2(b)]. The SQUIDs had outer dimensions 900 $\mu$m × 900 $\mu$m and hole dimensions 180 $\mu$m × 180 $\mu$m. The assembly was contained in a vacuum can surrounded by liquid helium that maintained the SQUIDs at 4.2 K. The sample was thermally isolated from the SQUIDs, and its temperature could be raised by means of a metal-film resistor. To avoid magnetic interaction between signals fed back to the SQUIDs, most of the data were obtained with the SQUIDs operated in an open loop. The experimental bandwidth was 0.6 Hz to 2.5 kHz.

We present results on $c$-axis oriented BSCCO and YBCO samples, with parameters specified in Table I. BSCCO (1) [12] and YBCO (1) [13] are thin films grown on substrates polished to thicknesses $<100$ $\mu$m. BSCCO

 0031-9007/95/74(14)/2796(4)$06.00 © 1995 The American Physical Society

(2) and (3) [14] and YBCO (2) and (3) [15] are single crystals. The crystal YBCO (3) had been irradiated with 1 GeV Au ions at a dose of $4.8 \times 10^8$ ions mm$^{-2}$ to introduce columnar defects along the $c$ axis [16]. For each sample, we obtained a measure of the diamagnetic shielding $S(T)$ ($0 \leq S \leq 1$) by determining the magnetic field required to induce one flux quantum in the SQUID; as the shielding decreases with increasing temperature, the required field is reduced. We define $T_0$ as the temperature at which $S(T)$ vanishes.

When the sample is cooled in a low applied magnetic field ($<10^{-7}$ T), vortex-antivortex pairs are generated at the superconducting transition; as the sample is cooled further, most of these vortices annihilate, but some are pinned and may hop among pinning sites under thermal activation. The characteristic time for this process is $\tau = \tau_0 \exp[U(T)/k_B T]$, where $\tau_0^{-1}$ is an attempt frequency, and $U(T)$ is the pinning energy that depends on the temperature $T$. This motion generates magnetic flux noise that is detected by the SQUIDs. We emphasize that each cooling process generates a different vortex configuration and thus possibly a different behavior at a given temperature. In general, we observe two distinct types of behavior [11]. The first consists of random telegraph signals (RTSs), in which the flux jumps randomly between two distinct values. The second is $1/f$ noise, where the spectral density scales as $1/f^\alpha$ with $\alpha$ close to unity, which is produced by an incoherent superposition of RTSs. At each temperature, RTSs produced by vortices with pinning energies within about $k_B T$ of a characteristic energy $\tilde{U}_0(\omega, T) = k_B T \ln(1/\omega\tau_0)$ contribute predominately to the spectral density of the flux noise at frequency $\omega$. Assuming $\tau_0 = 10^{-10}$ s, we find $\tilde{U}_0 = 21 k_B T$ for $\omega/2\pi = 1$ Hz. Thus, as the temperature is changed, different pinning sites with appropriate pinning energies are brought into the observable frequency range.

Figure 1 shows the time traces of two RTSs, in two different crystals, each measured simultaneously by the two SQUIDs. Also shown is the corresponding coherence $\gamma^2(f)$, defined by

$$\gamma^2(f) = |S_\Phi^{AB}(f)|^2 / S_\Phi^A(f) S_\Phi^B(f),$$

where $S_\Phi^A(f)$ and $S_\Phi^B(f)$ are the spectral densities of the flux noise measured by SQUIDs $A$ and $B$, and $S_\Phi^{AB}(f)$ is

TABLE I Parameters of samples.

| Sample | Type | Thickness ($\mu$m) | $T_0$ (K) |
|---|---|---|---|
| BSCCO (1) | Film | 0.075 | 76 |
| BSCCO (2) | Crystal | 4 | 88 |
| BSCCO (3) | Crystal | 29 | 81 |
| YBCO (1) | Film | 0.20 | 88 |
| YBCO (2) | Crystal | 30 | 90 |
| YBCO (3)[a] | Crystal | 30 | 90 |

[a]Columnar defects.

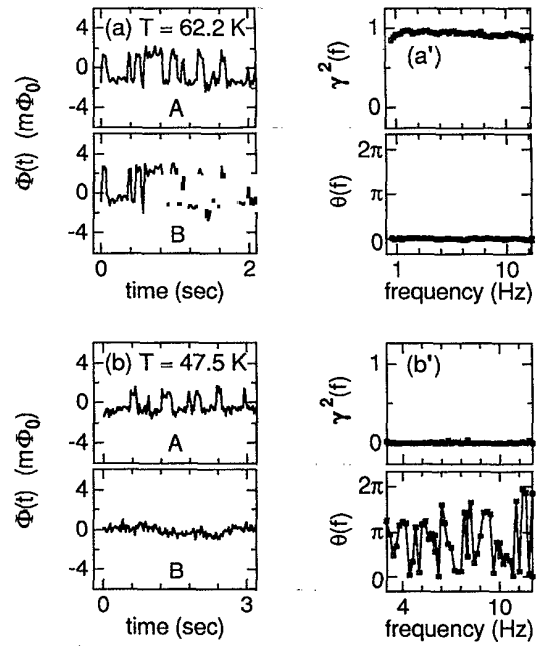


FIG. 1. Random telegraph signals detected by SQUIDs $A$ and $B$ for (a) YBCO (2) and (b) BSCCO (2); the corresponding coherences $\gamma^2(f)$ and relative phases $\theta(f)$ are shown in (a′) and (b′), respectively.

the cross-spectral density. The coherence varies from zero (no correlation) to unity (complete correlation). Finally, we show $\theta(f)$ ($0 \leq \theta \leq 2\pi$), the average relative phase of the two time traces [17]. In Fig. 1(a) [YBCO (2)], the two time traces show considerable correlation; this observation is confirmed in Fig. 1(a′), where $\gamma^2(f)$ is essentially unity and $\theta(f)$ is zero. we interpret this result as the hopping of a single vortex *as a rigid rod* between two pinning sites separated by at least 1.3 $\mu$m [11]. We observed comparable correlated RTSs in all of the BSCCO and YBCO crystals, and conclude that the rigidity of the vortices in both materials is high at least for time scales greater than 0.01 s. In all the crystals over certain temperature we also observe RTSs on one side with no corresponding RTSs on the other, so that $\gamma^2(f)$ is zero and $\theta(f)$ is randomly distributed; an example is shown in Fig. 1(b). This process is consistent with a vortex line that is strongly pinned near one end while the other end hops between two pinning sites.

For a given RTS, the hopping rate varies rapidly with temperature, so that it is observable only over a restricted temperature range. Thus, one typically observed a number of different RTSs over the temperature range of the experiment. For the limited number of RTSs we studied, correlated and uncorrelated processes occurred with approximately equal probability.

We turn now to a discussion of $1/f$ noise, which we observed in all samples at temperatures below the transition over the frequency range 0.6 Hz to 2.5 kHz, except over the narrow temperature ranges in which RTSs

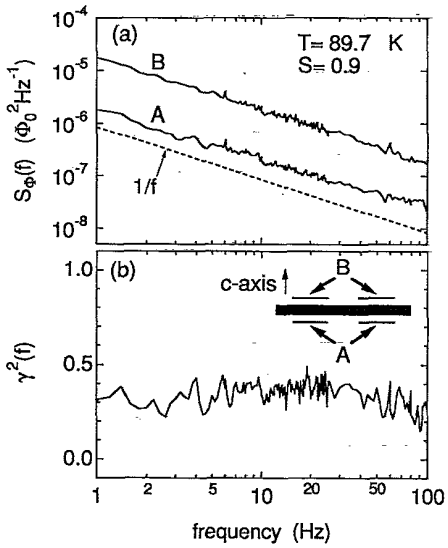


FIG. 2. (a) Spectral density of $1/f$ noise in YBCO (2) at 89.7 K, with $S(T) = 0.9$, measured by SQUIDs $A$ and $B$; (b) $\gamma^2(f)$ for the two spectra in (a). Inset shows configuration of experiment.

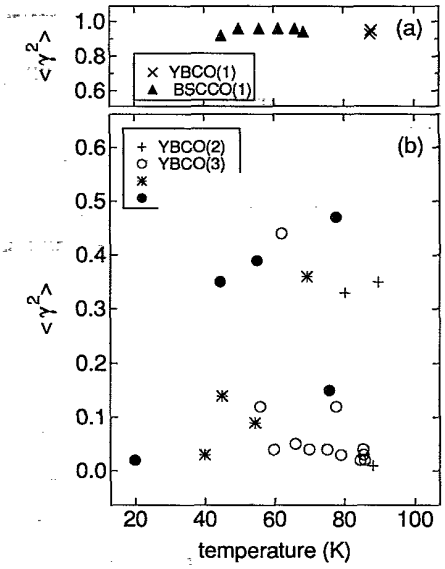


FIG. 3. $\langle\gamma^2\rangle$ vs temperature for $S \geq 0.9$ for (a) thin films and (b) thick crystals. The data for each sample were obtained from two to four separate thermal cyclings through $T_c$.

occurred. Figure 2 shows a representative example for YBCO (2) at 89.7 K with $S = 0.9$. The spectra measured by the two SQUIDs have slopes very close to $-1$ over the frequency range shown, 1–100 Hz, and $\gamma^2(f)$ is nearly white, with an average value $\langle\gamma^2\rangle = 0.35$.

We next briefly discuss the results from the thin films. Clem [18] has shown that when $\lambda_{ab}(T)$ exceeds the sample thickness, the motion of a pancake vortex at one surface will produce a nearly equal flux in both SQUIDs, giving a high degree of coherence. In Fig. 3(a) we plot $\langle\gamma^2\rangle$ vs temperature for films YBCO (1) and BSCCO (2), both with thicknesses less than or comparable to $\lambda_{ab}(T)$ [$\lambda_{ab}$(YBCO) $\approx$ 140 nm and $\lambda_{ab}$(BSCCO) $\approx$ 200 nm for the temperatures shown]; in both cases $S \geq 0.9$. The average $\langle\gamma^2\rangle$ is taken over the frequency range where $\gamma^2(f)$ is frequency independent [19]. The values of $\langle\gamma^2\rangle$ are essentially unity, with no temperature variation. This result is consistent with Clem's prediction, but does not resolve the issue of whether the vortices move as rigid rods or as independent pancakes, since both yield high coherence in the thin film limit.

Turning to the four crystals, we confine our attention to temperatures for which $S \geq 0.9$, thereby excluding temperatures near $T_0$, where $\lambda_{ab}(T)$ becomes greater than the sample thickness. In Fig. 3(b) we show $\langle\gamma^2\rangle$ vs temperature obtained from two to four thermal cyclings of each of the four samples. We note that many of the plotted values are near zero; however, the associated values of $\theta(f)$ are typically within $\pm 50°$ of 0°, implying that the coherence, although small, is indeed nonzero. In other cases $\langle\gamma^2\rangle$ is as high as 0.4. If we assume that each vortex has a probability $p$ to hop in a highly correlated manner [Fig. 1(a)] and $1 - p$ in an uncorrelated manner [Fig. 1(b)], then it can be shown that $\gamma^2(f) = p^2$ for the ensemble of RTSs generating $1/f$ noise. Thus, the value of $\langle\gamma^2\rangle = 0.4$ for $1/f$ noise suggests that about 60% of the vortices are moving as rigid rods at any given moment, while if we take a typical low value $\langle\gamma^2\rangle = 0.05$, about 20% have rigid rod behavior. Thus, even for $1/f$ noise with values of $\langle\gamma^2\rangle$ as low as 0.05, a significant fraction of the vortices contributing to the noise must have correlated motion.

A perusal of Fig. 3(b) shows that for a given sample $\langle\gamma^2\rangle$ has no systematic temperature dependence. Since the $1/f$ noise in a given frequency interval arises from progressively weaker pinning sites as the temperature is lowered, this result indicates that $p$ is not a monotonic function of the pinning energy. Furthermore, each thermal cycling yields a different value of $\langle\gamma^2\rangle$ at a given temperature, suggesting that processes with a given pinning energy have a variety of values of $p$. There is no significant difference between the coherence for the 4 and 29 $\mu$m thick BSCCO crystals, and no evidence for the coherence being higher in YBCO than in BSCCO, despite the fact that the predicted overall coupling energy between pancake vortices in adjacent layers is at least 50 times higher in YBCO. This behavior is complementary to results obtained in transport measurements on BSCCO [8,9], in which the force due to the current drives the vortices unidirectionally, causing them to shear. Lastly, the coherence in the columnar-defect YBCO crystal is similar to that observed in the other crystals, while its transport properties are vastly different [16].

In conclusion, we have shown that flux vortices as long as 30 $\mu$m along the $c$ axis in crystals of YBCO and BSCCO, cooled in nominally zero magnetic field

and in the absence of any driving current, can exhibit coherent motion for time scales greater than $10^{-2}$ s. The observation of both RTSs and $1/f$ noise indicate that typically 20% to 60% of the vortices exhibit such coherence. Both YBCO and BSCCO exhibited similar behavior, and there is no discernible dependence of the degree of coherence on sample thickness, temperature [provided $\lambda_{ab}(T) \ll$ sample thickness and $T < 0.9T_c$], or the presence of columnar defects. We interpret these results to imply that the differences between coherent and incoherent motion appear to be due to the distribution of pinning energies along the axis of flux line. When the flux line is pinned at a single site with a given pinning energy, it hops to another site as a rigid rod when given enough thermal energy. This means that thermal fluctuations alone are insufficient to disrupt the stack of pancake vortices, so that the lateral motion of a pancake at one point on a vortex can be transmitted to another point thousands of lattice spacings away. Conceivably, if the vortex is pinned at two or more sites with comparable energies, hopping at one site could induce hopping at another site. In contrast, when the flux line is pinned by at least one site with a much stronger pinning energy than any other pinning site along its length, then only part of the flux line is free to move at a given temperature, thereby producing incoherent motion. Thus, the flux lines in YBCO and BSCCO are flexible enough to bend at points of strong pinning, yet rigid enough to resist shearing due to thermal fluctuations. Finally, we believe that any effect of columnar defects on the coherence does not appear to low vortex densities, because the vortices whose motion we observe are mainly those pinned by native defects.

We are indebted to D. K. Christen, L. Krusin-Elbaum, and A. Marwick for performing the ion irradiation of the columnar-defect sample. This work was supported by the Director, Office of Energy Research, Office of Basic Energy Sciences, Materials Sciences Division of the U.S. Department of Energy under Contract No. DE-AC03-76SF00098 (T.S.L., N.M., L.T.S., and J.C.). Ames Laboratory is operated for the U.S. Department of Energy by Iowa State University under Contract No. W-7405-ENG-82. Fellowships from the National Science Foundation (T.S.L.), The Miller Institute for Basic Research in Science (N.M. and J.C.), and the Norwegian Research Council for Sciences and the Humanities (L.T.S.) are gratefully acknowledged.

*Present address: Sandia National Laboratories, Albuquerque, NM 87185.

†On leave from The Norwegian Institute of Technology, Division of Physics, N-7034, Trondheim, Norway.

[1] J. R. Chem, Phys. Rev. B **43**, 7838 (1991).

[2] M. V. Feigel'man, V. B. Beshkenbein, and A. I. Larkin, Physica (Amsterdam) **167C**, 177 (1990).

[3] A. Buzdin and D. Feinberg, J. Phys. (Paris) **51**, 1971 (1990).

[4] S. N. Artemenko and A. N. Kruglov, Phys. Lett. A **143**, 485 (1990).

[5] L. I. Glazman and A. E. Koshelev, Physica (Amsterdam) **173C**, 180 (1991).

[6] A. Kapitulnik, in *Phenomenology and Applications of High-Temperature Superconductors,* edited by K. S. Bedell, M. Inui, D. Meltzer, J. R. Schrieffer, and S. Doniach (Addison-Wesley, Reading, 1992), p. 34.

[7] J. R. Chem, Physica (Amsterdam) **200A**, 118 (1993).

[8] R. Busch, G. Ries, H. Werthner, G. Kreiselmeyer, and G. Saemann-Ischenko, Phys. Rev. Lett. **69**, 522 (1992).

[9] H. Safar, E. Rodriguez, F. de la Cruz, P. L. Gammel, L. F. Schneemeyer, and D. J. Bishop, Phys. Rev. B **46**, 14 238 (1992).

[10] H. Safar, P. L. Gammel, D. A. Huse, S. N. Majumdar, L. F. Schneemeyer, D. J. Bishop, D. Lopez, G. Nieva, and F. de la Cruz, Phys. Rev. Lett. **72**, 1272 (1994).

[11] M. J. Ferrari, M. Johnson, F. C. Wellstood, J. J. Kingston, T. J. Shaw, and John Clarke, J. Low Temp. Phys. **94**, 15 (1994).

[12] J. N. Eckstein, I. Bozovic, M. Klausmeier-Brown, G. F. Virshup, and K. S. Ralls, Thin Solid Films **216**, 8 (1992).

[13] K. Char, N. Newman, S. M. Garrison, R. W. Barton, R. C. Taber, S. S. Laderman, and R. D. Jacowitz, Appl. Phys. Lett. **57**, 409 (1990).

[14] L. W. Lombardo and A. Kapitulnik, J. Cryst. Growth **118**, 483 (1992).

[15] L. F. Schneemeyer, J. V. Waszczak, T. Siegrist, R. B. van Dover, L. W. Rupp, B. Batlogg, R. J. Cava, and D. W. Murphy, Nature (London) **328**, 601 (1987).

[16] L. Civale, A. D. Marwick, T. K. Worthington, M. A. Kirk, J. R. Thompson, L. Krusin-Elbaum, Y. Sun, J. R. Clem, and F. Holtzberg, Phys. Rev. Lett. **67**, 648 (1991).

[17] The frequency range has been cut off above 12 Hz. At higher frequencies, the white noise of the SQUID becomes significant, reducing the observed correlation.

[18] John R. Clem, Physica (Amsterdam) **235-240C**, 2607 (1994).

[19] Any frequency dependence of $\gamma^2(f)$ is usually caused by uncorrelated SQUID noise that becomes significant at frequencies where the sample noise is low.